

# Characterization of the structural transition in $\text{Na}_{0.75}\text{CoO}_2$

Q Huang<sup>1</sup>, J W Lynn<sup>1</sup>, B H Toby<sup>1</sup>, M-L Foo<sup>2</sup> and R J Cava<sup>2</sup>

<sup>1</sup> NIST Center for Neutron Research, NIST, Gaithersburg, MD 20899, USA

<sup>2</sup> Department of Chemistry, Princeton University, Princeton, NJ 08544, USA

Received 1 December 2004, in final form 11 February 2005

Published 11 March 2005

Online at [stacks.iop.org/JPhysCM/17/1831](http://stacks.iop.org/JPhysCM/17/1831)

## Abstract

In the  $\text{Na}_x\text{CoO}_2$  chemical system, a two-phase region is found at ambient temperature near  $x = 0.75$ . The manner in which that two-phase region is formed on cooling from a uniform single phase at temperatures above 340 K is reported here. The driving force that induces the phase separation appears to be a difference in Na composition of the two phases, which, though small, is accompanied by substantial differences in the unit cell parameters. Hysteretic behaviour in the transition is observed. One of the phases exhibits negative thermal expansion in the narrow temperature region where the phases are in the process of separating.

## 1. Introduction

$\text{Na}_x\text{CoO}_2$  has recently emerged as a unique example of a metallic conducting correlated electron system based on a layered triangular lattice. Superconductivity is observed [1] for hydrated materials at  $x = 0.3$ , a charge ordered insulator is observed [2] at  $x = 0.5$ , and an antiferromagnetic metal with a high thermoelectric power is observed [3, 4] at  $x = 0.7$ . These electronic phases occur in the context of changes in the crystal structure, which contains two  $\text{CoO}_2$  and two Na layers per unit cell [5–8]. The  $\text{CoO}_2$  layers consist of one triangular layer of Co sandwiched between two close packed layers of oxygen. Four chemical phases with different average crystal structures are observed in the range of compositions from  $x = 0.3$  to 1.0, as are a variety of different short range ordered Na arrangements [9–12]. The distinctions among the different phases are based primarily on the positions of the Na ions in the layers between the  $\text{CoO}_2$  layers, which occupy two kinds of sites. Na(1) is in a triangular prism that shares faces with  $\text{CoO}_6$  octahedra in the layers above and below, and Na(2) is in a triangular prism that shares edges with the  $\text{CoO}_6$  octahedra above and below. The Na(2) site triangular prism is occupied either by on-centre Na ions or displaced Na ions, depending on the total Na content [10–12]. For the hexagonal symmetry phase designated as H1, both Na sites are partially occupied, with the Na(2) displaced from the centres of the triangular prisms. This phase occurs over a wide range of Na content, from  $x = 0.3$  to 0.75, with the exception

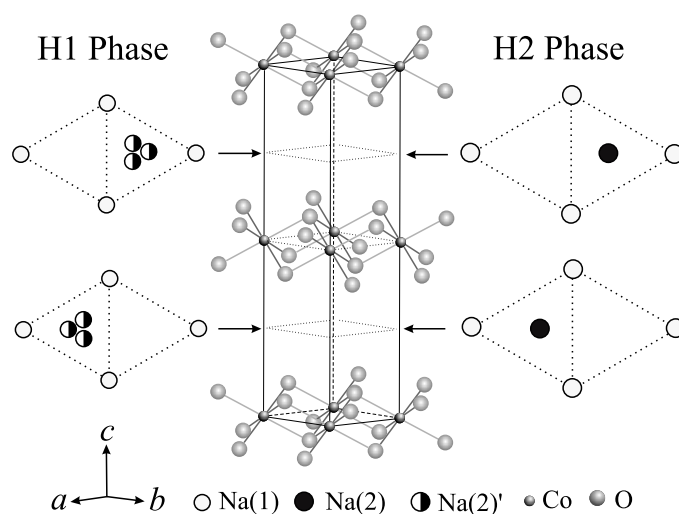


**Figure 1.** Structure models for  $\text{Na}_{0.75}\text{CoO}_2$ , space group  $P6_3/mmc$ . The structures consist of layers of edge-shared  $\text{CoO}_6$  octahedra in a triangular lattice (hexagonal unit cell,  $a_H \sim 2.85$  and  $a_H \sim 10.8$  Å), with Na ions occupying centred (H2 phase, right panel, with the Na(2) at the  $2c$  ( $2/3, 1/3, 1/4$ ) site) or off-centre (H1 phase, left panel, with the Na(2) at the  $6h$  ( $2x, x, 1/4$ ) site) positions in the interleaving planes.

of a charge ordered phase at exactly  $x = 0.5$  that has orthorhombic symmetry and zigzag chains of Na ions [13]. A second hexagonal symmetry phase, designated as H2, is found between  $x = 0.75$  and  $0.82$ . In the H2 phase, both the Na(1) and Na(2) sites are again partially occupied, but with the latter atoms in the centres of their triangular prisms rather than displaced. A comparison of the H1 and H2 phase structures is shown in figure 1. Finally, for  $\text{Na}_1\text{CoO}_2$ , the phase designated as H3, only the on-centre edge-sharing Na(2) site is occupied, with all possible sites of that type filled.

The thermodynamically stable composition range for  $\text{Na}_x\text{CoO}_2$  synthesized under normal conditions is between approximately  $x = 0.65$  and  $0.75$ . Crystals grown by the floating zone method most often have compositions near  $x = 0.75$ , and a narrow two-phase region is found at room temperature very close to that composition, with H1 and H2 phases in equilibrium [12]. Characterization of materials near ambient temperature (e.g. [14]) has sometimes revealed dramatic effects, suggesting the possible presence of an electronic phase transition in that temperature range. A crystal structure transition of the H2 structure type to the H1 structure type was later reported to occur on heating a sample which contained both H1 and H2 phases near  $x = 0.75$  [15] to temperatures just above ambient. The characterization of that phase transition in more detail is the subject of this paper. A very unusual combination of details is observed. The sample studied is stable as a mixture of H1 and H2 phases at temperatures below 340 K. In the temperature region of the phase transition that occurs just above room temperature, a significant amount of hysteresis is observed, implying that the structural transition is first order, yet the lattice parameters change in the temperature region where the relative proportion of phases is changing. Suggestions are made about the possible factors influencing the phase transition.

## 2. Experimental details

The powder sample was prepared by heating  $\text{Na}_2\text{CO}_3$  and  $\text{Co}_3\text{O}_4$  in the appropriate proportions in oxygen at  $800^\circ\text{C}$  overnight. The neutron powder diffraction intensity data for  $\text{Na}_{0.75}\text{CoO}_2$

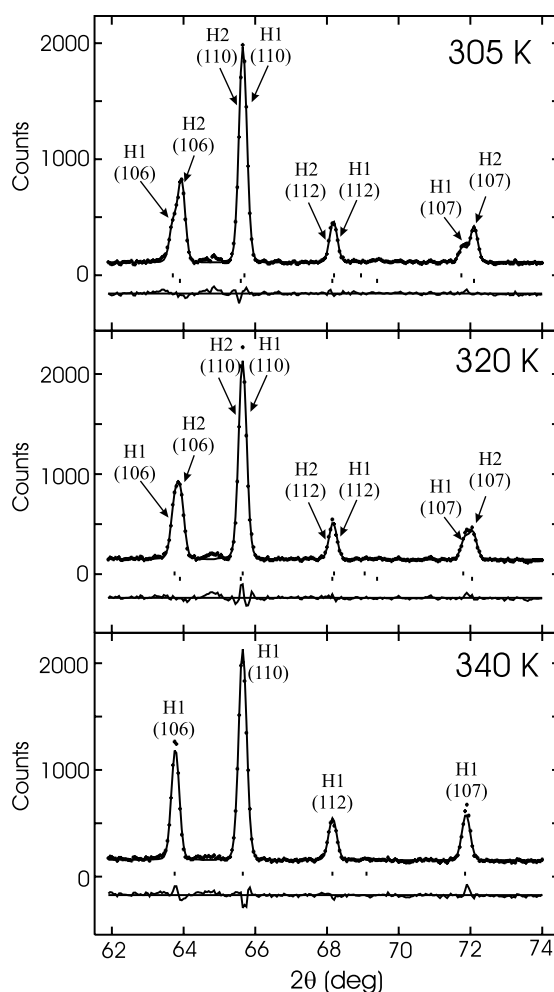


**Figure 2.** Portion of the observed (crosses) and calculated (solid curve) neutron powder diffraction patterns for  $\text{Na}_{0.75}\text{CoO}_2$ . Intensities observed at 305 and 320 K were fitted using a two-phase (H1 + H2) model, and a single-phase (H1) model was used to fit the intensities at 340 K.

were collected using the BT-1 high resolution powder diffractometer at the NIST Center for Neutron Research, employing a Cu(311) monochromator to produce a monochromatic neutron beam of wavelength 1.5403 Å. Collimators with horizontal divergences of 15', 20', and 7' of arc were used before and after the monochromator, and after the sample, respectively. The intensities were measured in steps of 0.05° in the  $2\theta$  range 3°–168°. In order to study the structural transition, the neutron diffraction data were collected at a series of temperatures between 3.5 and 400 K. The structural parameters were refined using the program GSAS [16]. The neutron scattering amplitudes used in the refinements were 0.363, 0.253, and 0.581 ( $\times 10^{-12}$  cm) for Na, Co, and O, respectively.

### 3. Results and discussion

The observed neutron diffraction pattern in the vicinity of the (107) group of reflections at 305, 320, and 340 K is shown in figure 2. At 305 K (and for all lower temperatures) two

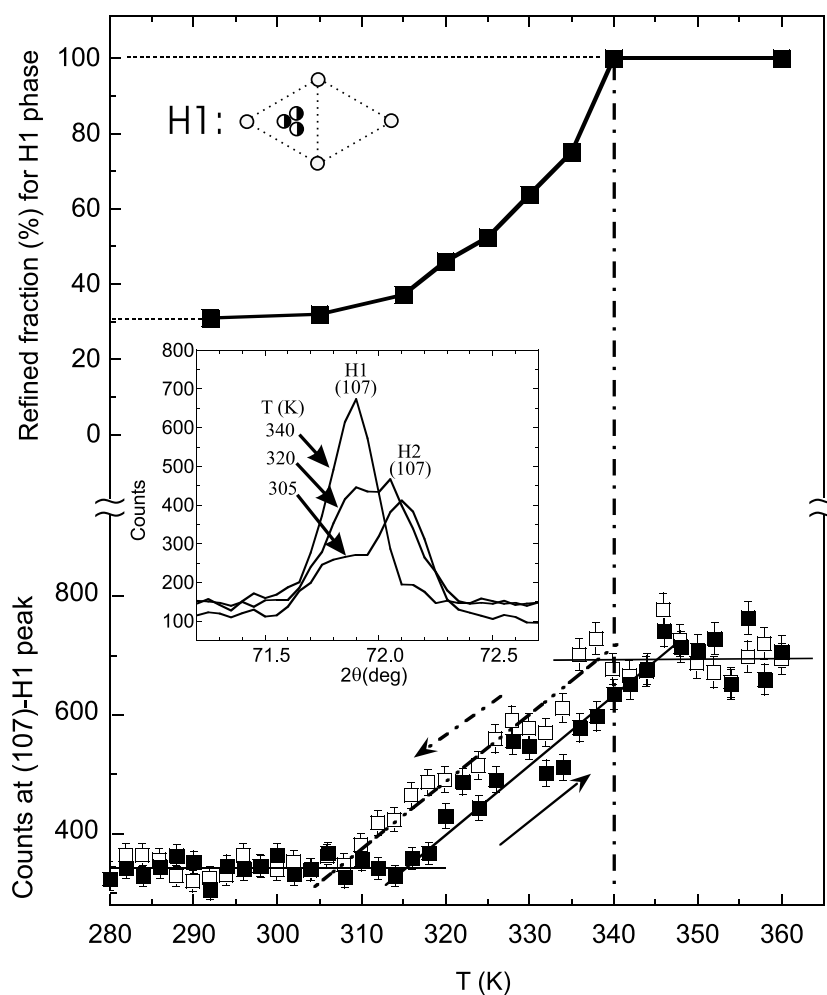


**Figure 3.** Refined fraction of the H1 phase and the peak counts at the H1 phase (107) peak position as a function of temperature, indicating that a reversible phase separation occurs between 310 and 340 K. Below 310 K the phase fractions remain constant to low temperature. The 5 K hysteresis in the phase transition is shown in the difference between the 107 peak intensities on heating and cooling. The inset shows a single (107) peak, and hence the presence of a single phase above  $\sim 340$  K.

(107) peaks are observed, at  $2\theta = 71.9^\circ$  and  $72.1^\circ$ , with an intensity ratio of approximately 1:2. Full refinements demonstrate that these two peaks belong to two different phases, having the H1 and H2 structures. At 320 K the intensity of the (107)-H2 peak has decreased, and it is unobservable at 340 K. On the other hand, the (107)-H1 peak intensity increases with increasing temperature. At 340 K the full width at half-maximum (FWHM) of the (107) peak from the H1 phase is  $0.24(1)^\circ$ , which is the instrumental resolution. This indicates that it is a single peak, and therefore that the sample is single phase at and above 340 K.

Monitoring the changes in the H1 phase (107) peak intensity (figure 3) indicates that a reversible phase separation of a single H1 phase into H1 plus H2 phases occurs on cooling between 340 and 310 K. The intensity variation with temperature and the phase fractions obtained from the structure refinements demonstrate that two well-formed structural phases

are present rather than a structural distortion of a single phase. The growth of the H2 phase on cooling is shown in the increase in intensity of its (107) peak, seen in the inset to figure 3. A structural refinement employing diffraction data collected at 3.5 K indicated that the phase fractions are temperature independent from 305 to 3.5 K.

The refined structural parameters for the H1 and H2 phases at representative temperatures are given in table 1. Figure 2 shows the agreement of the refined two-phase structural models to the data. Both phases have  $P6_3/mmc$  symmetry and a hexagonal lattice with  $a_H \sim 2.8$  and  $c_H \sim 10.8$  Å. In the H2 phase, the Na(2) is at the central  $2c$  ( $2/3, 1/3, 1/4$ ) site, and in the H1 phase the Na(2) is randomly positioned at one of three symmetrically located off-centre  $6h$  ( $2x, x, 1/4$ ) sites in the interleaving planes.

The refined cell parameters for the H1 and H2 phases as a function of temperature are shown in figure 4. The H1 phase, starting in the single-phase region at higher temperatures, shows the expected shrinkage of cell parameters with decreasing temperature. On cooling to below 340 K, the H2 phase appears with increasing relative fraction between the temperatures 340 and 310 K. This region of the diagram is hysteretic, as seen in figure 3. In this two-phase region, accompanying the increasing fraction of the H2 phase on cooling, the cell parameters of the two phases change with temperature. The cell parameters and volume of the H2 phase behave in the expected manner on cooling: shrinking with decreasing temperature. The H1 phase, however, undergoes anomalous negative thermal expansion in the temperature region where the relative fractions of the two phases is changing.

Characterization of the Na sublattice as a function of composition provides the structural basis for distinguishing the different chemical phases in the Na<sub>*x*</sub>CoO<sub>2</sub> phase diagram. Therefore the characterization of that sublattice in Na<sub>0.75</sub>CoO<sub>2</sub> as a function of temperature is of interest. The upper panel of figure 5 shows the Na compositions of the H1 and H2 phases obtained on cooling from the single-phase H1 at temperatures above 340 K. This panel shows that there is indeed a compositional phase separation that occurs when the H1 and H2 phases separate on cooling. The difference in composition for the two phases formed is very small, at the limits of our experimental precision. From a uniform H1 phase above 340 K at  $x = 0.75$  in Na<sub>*x*</sub>CoO<sub>2</sub>, two phases are formed on cooling, one with a slightly lower Na content (about  $x = 0.72$ ) and one with a slightly higher Na content (about  $x = 0.76$ ). Although this differentiation in Na content is the most likely underlying cause for the phase separation, it is quite a subtle difference. The middle panel of figure 5 shows that the Na–O bond distances for the Na(1) atoms in both H1 and H2 phases, and the Na–O distances for the Na(2) atoms in the H2 phase do not change substantially in the phase separation temperature region. The lower panel, however, shows that the Na–O bond lengths in the H1 phase for the off-centre Na(2) atom change significantly in the temperature region of the phase separation. The Na(2) atom moves substantially more off-centre on cooling as the phase separation proceeds to completion below 340 K. This may be in response to the developing chemical differentiation between the two phases on cooling, but could be driven by other forces.

The structural refinements for the ambient temperature Na<sub>*x*</sub>CoO<sub>2</sub> phase diagram indicated that the thickness of the CoO<sub>2</sub> layer changed significantly across the compositional diagram between  $x = 0.3$  and 1.0 [12]. This layer thickness is of interest because it directly reflects the aspect ratio of the CoO<sub>6</sub> octahedra, which in turn is likely to have a strong influence on the energies of the Co  $t_{2g}$  orbitals at the Fermi energy. Figure 6 shows the characterization of the Co–O system in Na<sub>0.75</sub>CoO<sub>2</sub> as a function of temperature in the vicinity of the phase separation. Bond lengths, bond angles, and the fractional thickness of the CoO<sub>2</sub> layer compared to the thickness of a layer made of ideal octahedra are plotted. The figure shows that systematic changes are observed for the CoO<sub>2</sub> sublattice in the H1 phase, though they are at the limit of our experimental precision. The Co–O bond lengths decrease on cooling, and the O–Co–O

**Table 1.** Structure parameters of Na<sub>0.75</sub>CoO<sub>2</sub> at 305, 320, and 340 K. Space group  $P6_3/mmc$ , atomic positions: Co: 2a (0 0 0); Na(1): 2b (0 0 1/4); Na(2): 6h (2x, x, 1/4) for the H1 phase or 2c (2/3, 1/3, 1/4) for the H2 phase; O: 4f (1/3, 2/3, z). There is ~0.4 wt% CoO impurity.

<i>T</i> (K)	305		320		325		330		340
<i>x</i> (refined)	0.72(3)	0.75(2)	0.75(2)	0.76(3)	0.74(3)	0.75(4)	0.73(2)	0.76(4)	0.75(1)
Phase & fraction (%)	H1(31.8(3))	H2(67.7(2))	H1(45.4(4))	H2(54.1(4))	H1(52.1(2))	H2(47.4(5))	H1(64.2(4))	H2(35.6(6))	H1(100)
<i>a</i> (Å)	2.8376(1)	2.84073(7)	2.8387(1)	2.8415(1)	2.8389(1)	2.8419(1)	2.83904(9)	2.8422(1)	2.83940(9)
<i>c</i> (Å)	10.8738(5)	10.8122(3)	10.8629(5)	10.8164(4)	10.8619(5)	10.8174(5)	10.8586(5)	10.8163(7)	10.8545(3)
<i>V</i> (Å <sup>3</sup> )	75.827(6)	75.562(4)	75.809(6)	75.630(5)	75.811(6)	75.662(6)	75.796(5)	75.670(6)	75.838(5)
Co <i>B</i> (Å <sup>2</sup> )	0.30(4)	0.30(4)	0.27(4)	0.27(4)	0.26(4)	0.26(5)	0.26(4)	0.26(4)	0.29(4)
Na(1) <i>B</i> (Å <sup>2</sup> )	1.1(1)	1.1(1)	1.1(1)	1.1(1)	1.3(2)	1.3(5)	1.4(2)	1.4(2)	1.7(2)
<i>n</i>	0.183(21)	0.204(12)	0.188(20)	0.224(18)	0.166(19)	0.213(21)	0.151(16)	0.271(29)	0.193(16)
Na(2) <i>x</i>	0.272(3)		0.283(3)		0.283(3)		0.294(3)		0.291(2)
<i>B</i> (Å <sup>2</sup> )	1.1(1)	1.1(1)	1.1(1)	1.1(1)	1.3(2)	1.3(2)	1.4(2)	1.4(2)	1.2(2)
<i>n</i>	0.178(10)	0.543(15)	0.188(8)	0.536(20)	0.191(8)	0.537(24)	0.191(6)	0.485(30)	0.185(4)
O <i>z</i>	0.0901(3)	0.0913(1)	0.0905(2)	0.0913(2)	0.0906(2)	0.0912(2)	0.0906(2)	0.0911(3)	0.0907(1)
<i>B</i> (Å <sup>2</sup> )	0.56(2)	0.56(2)	0.51(2)	0.51(2)	0.61(3)	0.61(3)	0.65(2)	0.65(2)	0.52(2)
<i>R<sub>p</sub></i> (%)		6.01		5.66		5.93		5.74	5.92
<i>R<sub>wp</sub></i> (%)		7.42		7.09		7.28		7.08	7.35
$\chi^2$		1.001		1.068		1.072		0.9952	1.198

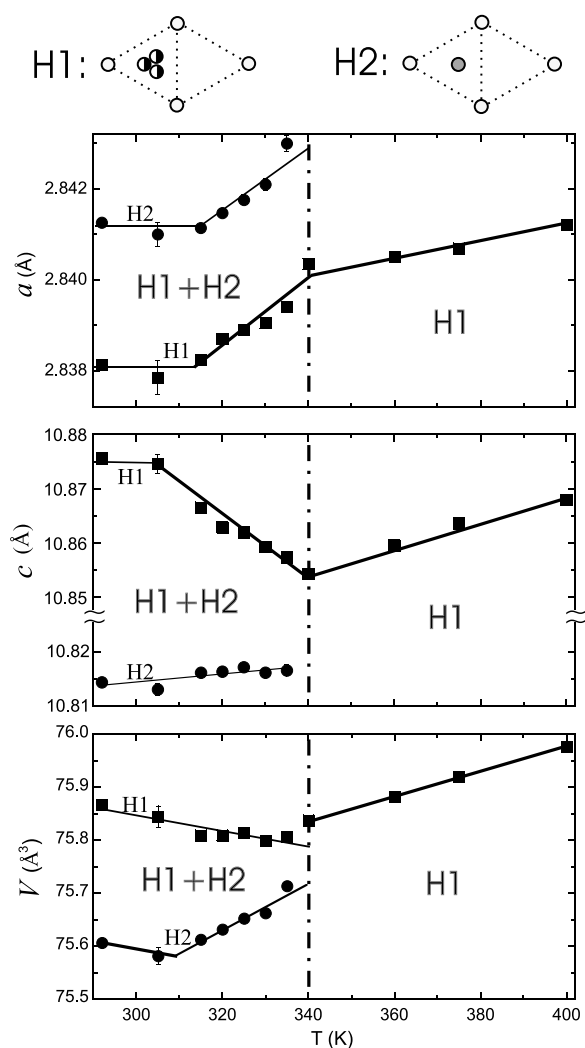


**Figure 4.** The temperature dependence of the lattice parameters and unit cell volumes for  $\text{Na}_{0.75}\text{CoO}_2$  in the single-phase and two-phase regions. The lattice parameters of the H1 and H2 phases are distinctly different, and the temperature dependence of the  $c$  axis parameter of the H1 phase, and its volume, are highly anomalous in the temperature range where the phase separation is occurring.

bond angle increases. The net effect of the combination of these two changes leaves the relative thickness of the octahedron relatively unchanged. For the H2 phase, no clearly discernible systematic changes are observed to within our precision.

#### 4. Conclusions

The structural two-phase region between the H1 and H2 phases in the  $\text{Na}_x\text{CoO}_2$  phase diagram at room temperature disappears on heating to temperatures above 340 K. Above that temperature a single phase of the H1 type is found. The H1 phase region that extends between  $x = 0.3$  and  $0.75$  at ambient temperature therefore extends to higher Na contents at

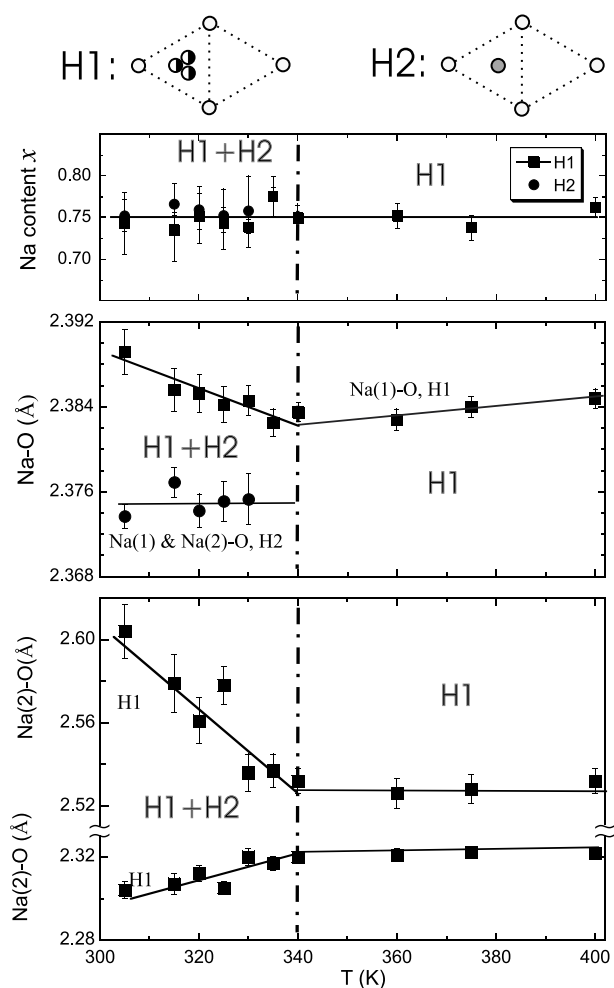


**Figure 5.** Characterization of the Na sublattice in  $\text{Na}_{0.75}\text{CoO}_2$  as a function of temperature in the vicinity of the phase separation. Upper panel, the Na compositions of the H1 and H2 phases. Middle panel, the Na–O bond distances for Na(1) (the prismatic site that shares faces with the  $\text{CoO}_6$  octahedra) in both H1 and H2 phases, and the Na–O distances for Na(2) centred in the triangular prisms (the prismatic site that shares edges with the  $\text{CoO}_6$  octahedra) in the H2 phase. The lower panel shows the substantial change in the Na–O bond lengths in the H1 phase, where the Na(2) atom is off-centre in its triangular prism. This panel shows that the Na(2) atom moves continuously more off-centre as the phase separation proceeds below 340 K.

temperatures just above ambient. It would be of interest to follow the stability of the H1 phase at high temperatures as the Na content is increased beyond  $x = 0.75$ . There is a relatively wide two-phase region between H2 and H3 phases centred around  $x = 0.8$  at room temperature that must therefore evolve to an H1–H3 two-phase region at higher temperatures.

At first sight, the driving force for the phase separation near  $x = 0.75$  is a compositional disproportionation between the higher Na content H2 and lower Na content H1 phases. The difference in the Na sites occupied in these two phases (off-centre Na(2) in the H1 phase and on-centre Na(2) in the H2 phase) drives a difference in their lattice parameters perpendicular to the  $\text{CoO}_2$  planes that lends a substantial first-order character to the phase separation. However,

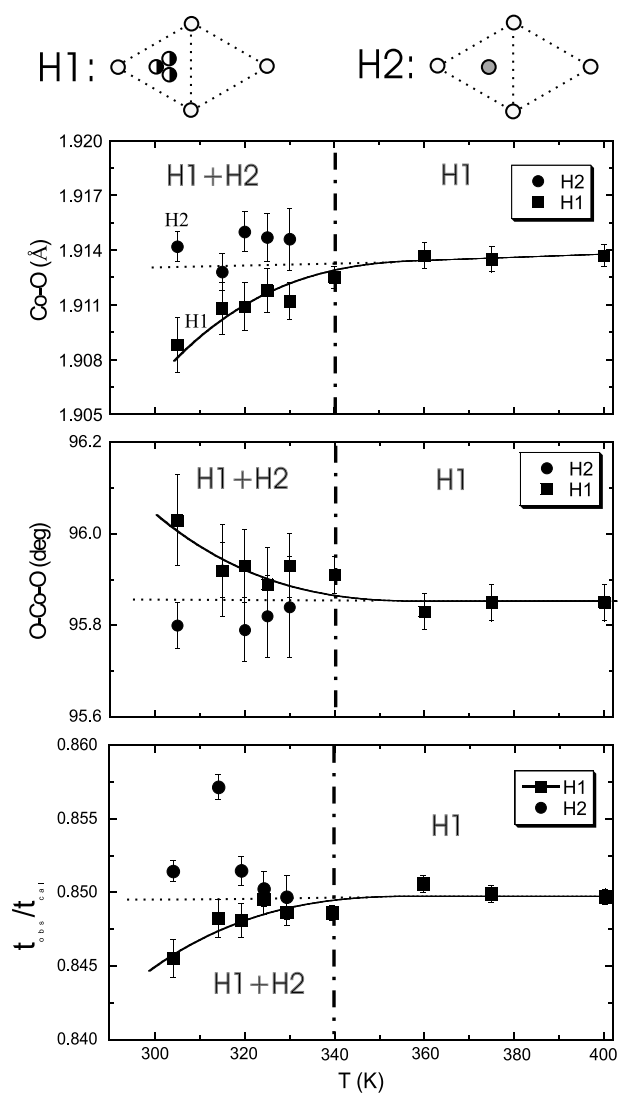


**Figure 6.** Characterization of the Co–O system in  $\text{Na}_{0.75}\text{CoO}_2$  as a function of temperature in the vicinity of the phase separation. The lower panel shows the ratio of the thickness of the  $\text{CoO}_2$  layer compared to the thickness that would be found if the  $\text{CoO}_6$  octahedra had an ideal shape.

the continuous changes in the structural parameters in the H1 phase in the temperature region where the phase separation occurs indicate that there is substantial second-order character present as well. The anomalous behaviour of the cell parameters and cell volume in the H1 phase on cooling in the vicinity of the phase separation suggests that there may be strain in the system due to the significant volume differences between the two phases that affects the manner in which the phase separation takes place.

### Acknowledgments

The work at Princeton was supported by the US Department of Energy and The National Science Foundation, grants DE-FG02-98-ER45706 and NSF-DMR-0213706.

## References

- [1] Takada K, Sakurai H, Takayama-Muromachi E, Izumi F, Dilanian R A and Sasaki T 2003 *Nature* **422** 53
- [2] Foo M L, Wang Y, Watauchi S, Zandbergen H W, He T, Cava R J and Ong N P 2004 *Phys. Rev. Lett.* **92** 247001
- [3] Terasaki I, Sasago Y and Uchinokura K 1997 *Phys. Rev. B* **56** R12685
- [4] Wang Y, Rogado N S, Cava R J and Ong N P 2003 *Nature* **423** 425
- [5] Delmas C, Braconnier J J, Fouassier C and Hagenmuller P 1981 *Solid State Ion.* **3/4** 165
- [6] Fouassier C, Matejka G, Reau J-M and Hagenmuller P 1973 *J. Solid State Chem.* **6** 532
- [7] Ono Y, Ishikawa R, Miyazaki Y, Ishii Y, Morii Y and Kajitani T 2002 *J. Solid State Chem.* **66** 177
- [8] Balsys R J and Davis R L 1996 *Solid State Ion.* **93** 279
- [9] Foo M L, Xu Q, Kumar V, Cava R J and Zandbergen H W 2004 *Phys. Rev. B* **70** 024101
- [10] Jorgensen J D, Avdeev M, Hinks D G, Burley J C and Short S 2003 *Phys. Rev. B* **68** 214517
- [11] Lynn J W, Huang Q, Brown C M, Miller V L, Foo M L, Schaak R E, Jones C Y, Mackey E A and Cava R J 2003 *Phys. Rev. B* **68** 214516
- [12] Huang Q, Foo M L, Pascal R A Jr, Lynn J W, Toby B H, He T, Zandbergen H W and Cava R J 2004 *Phys. Rev. B* **70** 184110
- [13] Huang Q, Foo M L, Lynn J W, Zandbergen H W, Lawes G, Wang Y, Toby B, Ramirez A P, Ong N P and Cava R J 2004 *J. Phys.: Condens. Matter* **16** 5803
- [14] Gavilano J L, Rau D, Pedrini B, Hinderer J, Ott H R, Kazakov S M and Karpinski J 2004 *Phys. Rev. B* **69** 100404
- [15] Huang Q, Khaykovich B, Chou F C, Cho J H, Lynn J W and Lee Y S 2004 *Phys. Rev. B* **70** 134115
- [16] Larson A and Von Dreelle R B 1994 *Los Alamos National Laboratory, Internal Report*